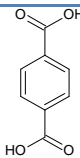
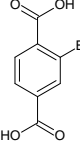
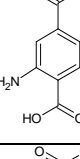
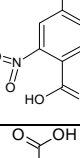
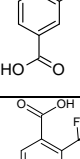
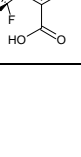


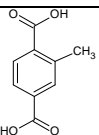
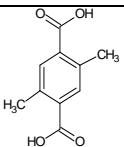
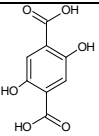
Supplementary Information (SI)

1. Synthesis of UiO-66's solids

The synthesis of the UiO-66 materials was performed under solvothermal conditions following a modified procedure of the previously reported protocol^{1,2,3,4,5} Typically, 1 mmol of zirconium (IV) chloride (ZrCl₄) and 1 mmol of the dicarboxylic linker were dispersed in 3 mL of dimethylformamide (DMF), placed in a Teflon-lined autoclave and heated at different temperatures (Table S1). The resulting solid was recovered by filtration and washed with deionized water and acetone. After filtration, the activation was carried out by solvent exchange in order to remove the remaining organic ligand and/or solvent. Indeed, 200 mg of the solid were suspended in 100 mL of DMF under stirring for 12 h. Then, the DMF-washed solid was suspended in 100 mL of MeOH under stirring for 12 h, recovering the activated solid by filtration.

Table S1. Synthesis conditions of the UiO-66s(Zr).

UiO-66	Linker	Time (h)@ Temperature (°C)
H		12@220
Br		20@100
NH ₂		24@100
NO ₂		24@220
Cl		24@100
2CF ₃		24@100

CH₃		24@100
2CH₃		24@100
2OH		24@130

*MeOH = methanol; DMF = dimethylformamide

2. Drug encapsulation

Caffeine was entrapped into the UiO-66 solids by suspending the powder samples in 10 mL of a 10 mg·mL⁻¹ aqueous caffeine solution or 20mg·mL⁻¹ ibuprofen solution in ethanol, at room temperature under magnetic stirring for 72 hours. The ratio material: drug weight was 1:2 (caffeine) and 1:4 (ibuprofen). The drug-containing solids were recovered by filtration and dried at room temperature. The adsorbed drug amount was quantified by thermogravimetric analysis (TGA), high performance liquid chromatography (HPLC) and elemental analysis (EA). The solids before and after the drug entrapping were characterized by X-Ray Powder Diffraction (XRPD), Infrared Spectroscopy and N₂ adsorption isotherms.

X-Ray Powder Diffraction (XRPD)

The XRPD patterns were collected using a SIEMENS D5000 diffractometer (θ -2 θ) with a Cu K α 1 radiation ($\lambda = 1.54056$ angstroms) from 5 to 15° (2 θ) and a step size of 0.04° and 4 s per step in continuous mode (Figure S1).

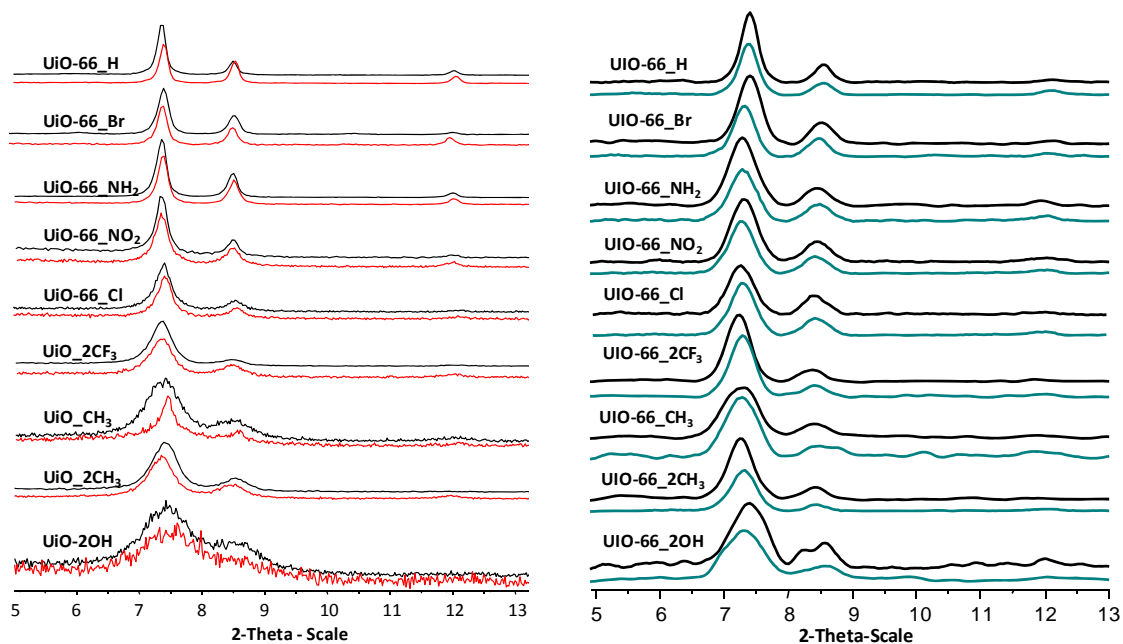
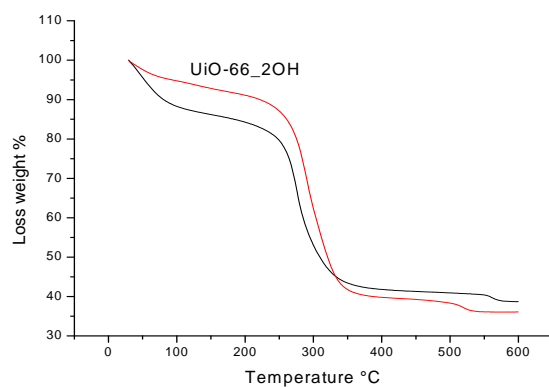
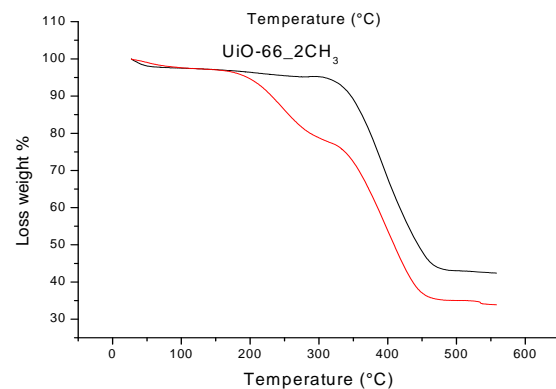
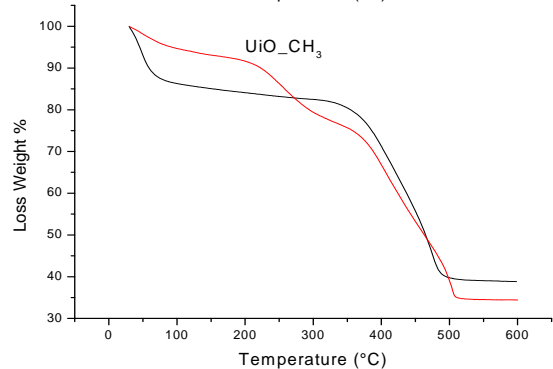
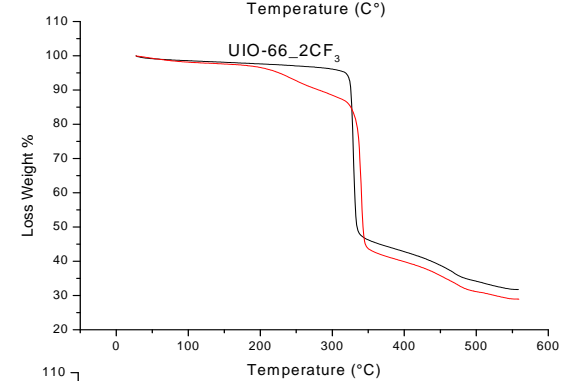
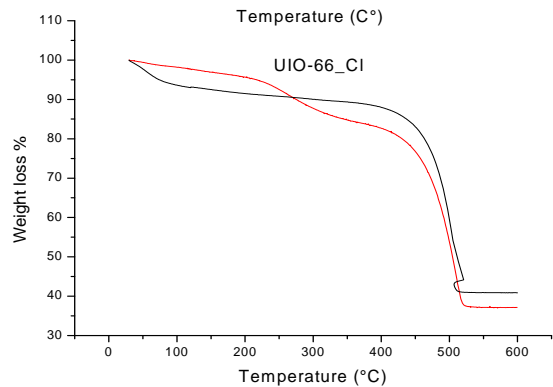
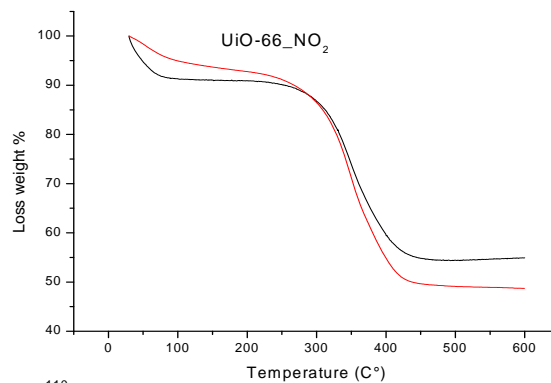
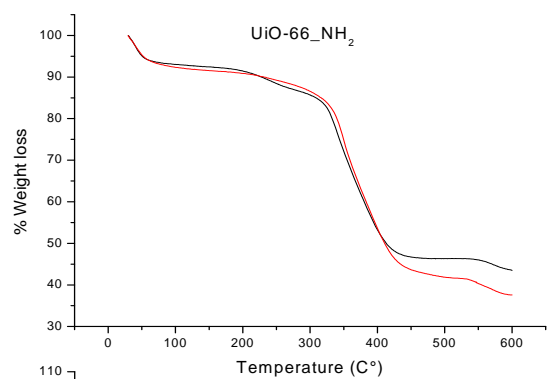
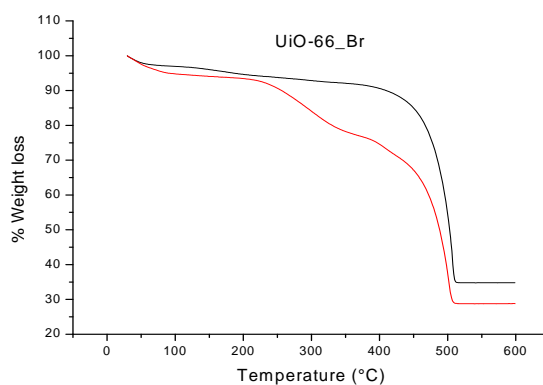
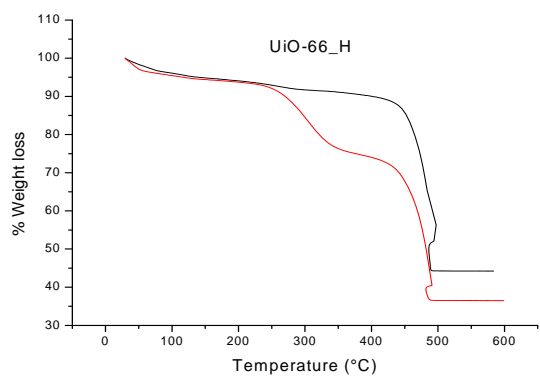


Figure S1. XRPD patterns of starting solids (black), caffeine-loaded (red), and ibuprofen loaded-materials (green)

Thermogravimetric analysis (TGA)

The samples (5-10 mg) were analysed under an oxygen flow ($20 \text{ mL}\cdot\text{min}^{-1}$) using a Perkin Elmer Diamond TGA/DTA STA 6000 running from room temperature to $600 \text{ }^\circ\text{C}$ with a scan rate of $2 \text{ }^\circ\text{C}\cdot\text{min}^{-1}$. Typically, caffeine or ibuprofen containing samples show three different weight losses. The first weight loss, between 30 and 150°C , is due to the departure of water, the second one more or less differentiated (from around 150 to 300°C) corresponds to the API departure and the last one (300 - 550°C) is related to the linker departure, so the degradation of the hybrid solid (Figure S2).



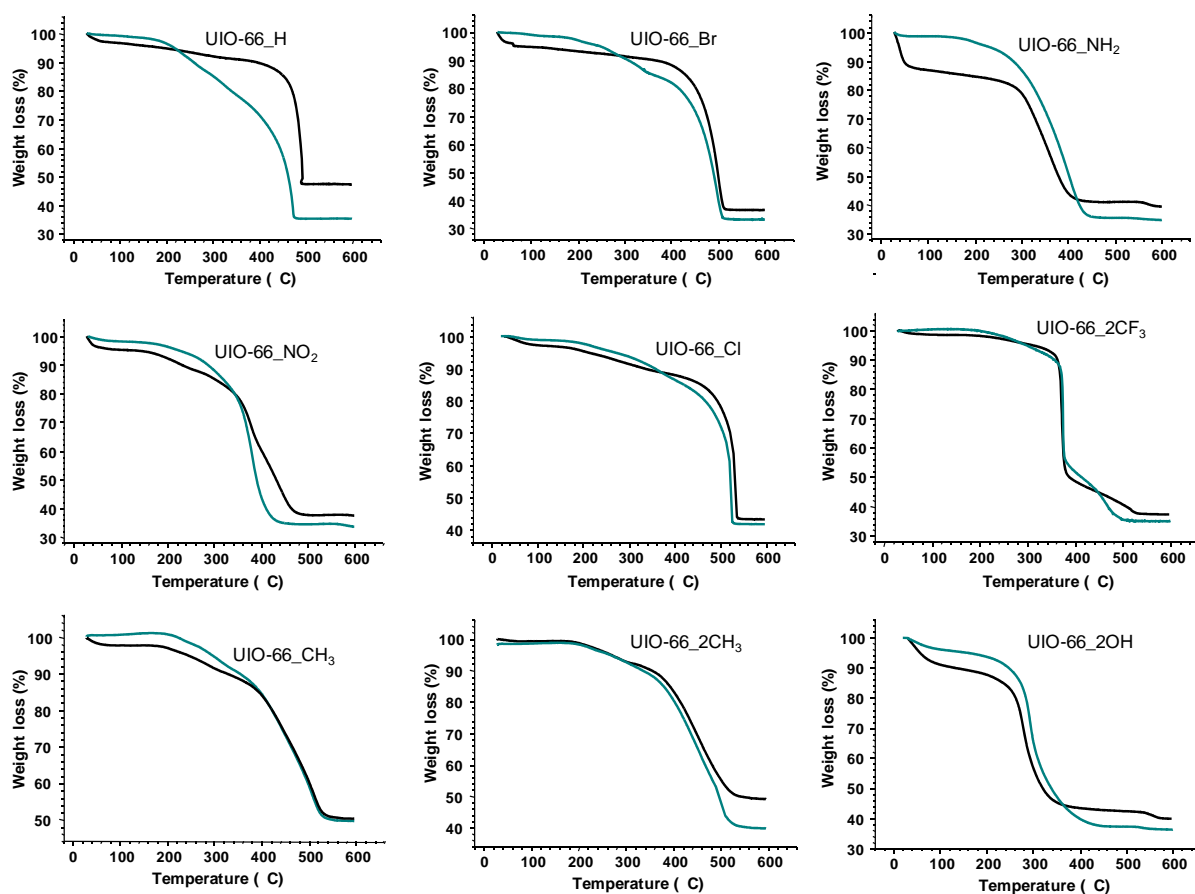


Figure S2.TGA of the starting MOF samples (black), caffeine-loaded (red) and ibuprofen-loaded materials (green)

N₂ adsorption isotherms

The N₂ isotherms were obtained at 77K using a Belsorp Mini (Bel, Japan). Prior to the analysis, approximately 40-60 mg of UiO-66 samples were evacuated for 12-24 h at 200°C under vacuum for the bared materials, or 80°C for the API loaded solids (Figure S3).

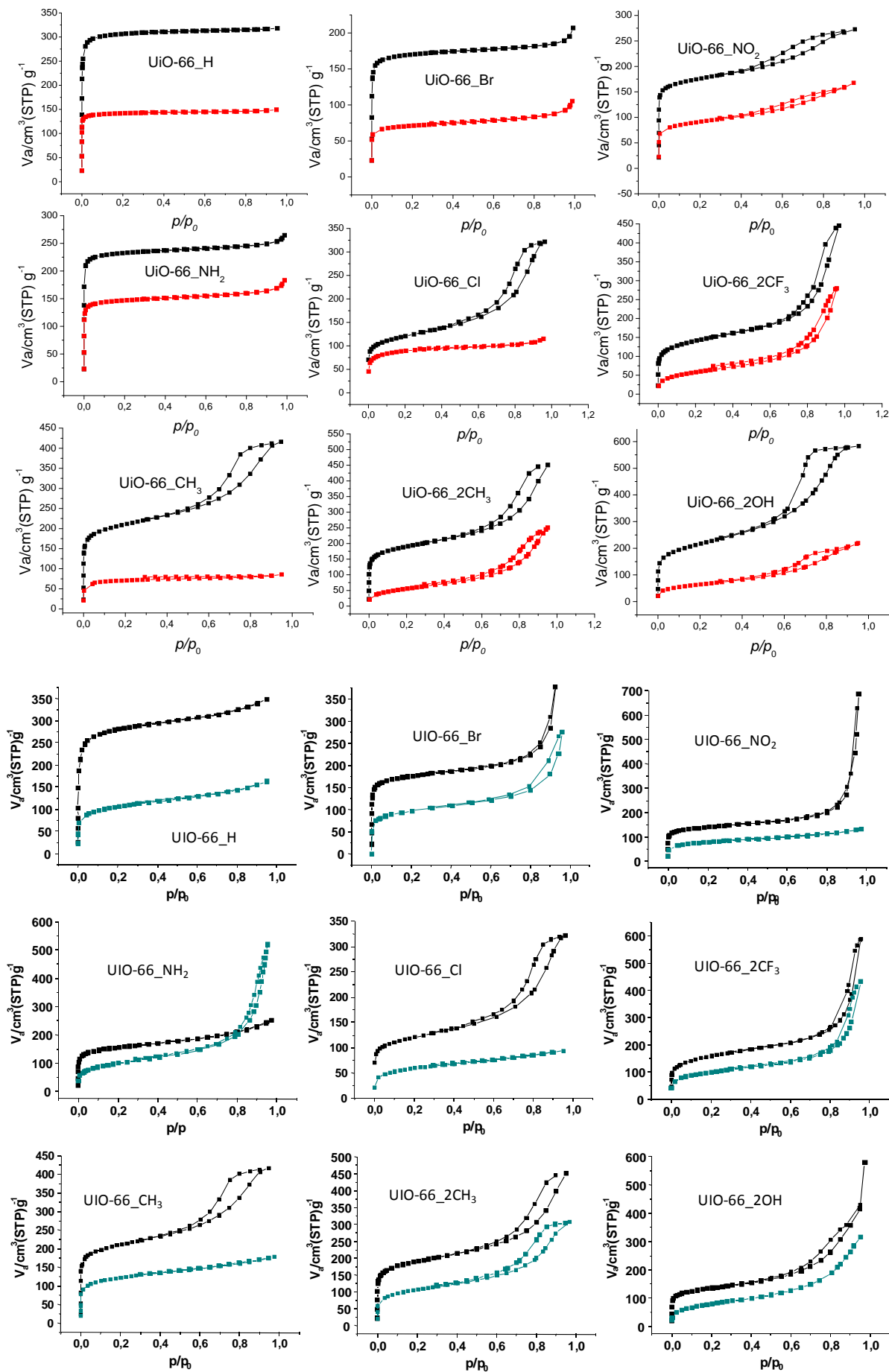


Figure S3. Nitrogen adsorption isotherms at 77 K for the starting materials (black), caffeine-loaded materials (red, on top) and ibuprofen-loaded ones (green, on the bottom).

Table S2. Pore volume and BET surface area of the starting UiO-66 materials, the caffeine-containing UiO-66 and the ibuprofen-loaded UiO-66.

UiO-66	Starting material		Caffeine-loaded		Ibuprofen-loaded	
	V_{microp} ($\text{cm}^3 \cdot \text{g}^{-1}$)	S_{BET} ($\text{m}^2 \cdot \text{g}^{-1}$)	V_{microp} ($\text{cm}^3 \cdot \text{g}^{-1}$)	S_{BET} ($\text{m}^2 \cdot \text{g}^{-1}$)	V_{microp} ($\text{cm}^3 \cdot \text{g}^{-1}$)	S_{BET} ($\text{m}^2 \cdot \text{g}^{-1}$)
H	0.48	1230	0.22	570	0.11	361
CH ₃	0.34	760	0.11	265	0.23	479
2CH ₃	0.31	680	0.10	203	0.18	447
2CF ₃	0.24	503	0.10	210	0.07	247
Br	0.30	640	0.11	270	0.14	322
Cl	0.23	430	0.15	320	0.12	230
NO ₂	0.28	660	0.15	330	0.14	251
NH ₂	0.35	930	0.22	580	0.03	334
2OH	0.30	755	0.12	315	0.06	288

High performance liquid chromatography (HPLC) determination

The amount of encapsulated and released API as well as the release of the organic linker were determined using a reversed phase HPLC system Waters Alliance E2695 separations module (Waters, Milford, MA, USA), equipped with a variable-wavelength photodiode array detector Waters 2998 and controlled by Empower software.

Sunfire-C₁₈ reverse-phase column (5 μm , 4.6x150 mm Waters) was employed. The mobile phase consisted of 40% solution (v/v) of methanol in phosphate buffer solution (PBS) 0.04 M pH 2.5 for caffeine and 85% solution (v/v) of methanol in PBS 0.04M pH 2.5 for ibuprofen. The flow rate was 1 $\text{mL} \cdot \text{min}^{-1}$ (caffeine) or 0.8 $\text{mL} \cdot \text{min}^{-1}$ (ibuprofen) and the column temperature was fixed at 25°C. The injection volume was 50 μL . Several ethanol caffeine solutions (0, 1.5, 3, 3.75, 6, 7.5, 15 and 30 $\mu\text{g} \cdot \text{mL}^{-1}$) and ethanol ibuprofen solutions (0.001, 0.003, 0.004, 0.005, 0.006, 0.008, 0.01, 0.02, 0.03, 0.05 and 0.1 $\text{mg} \cdot \text{mL}^{-1}$) were used as standards (Figure S4)

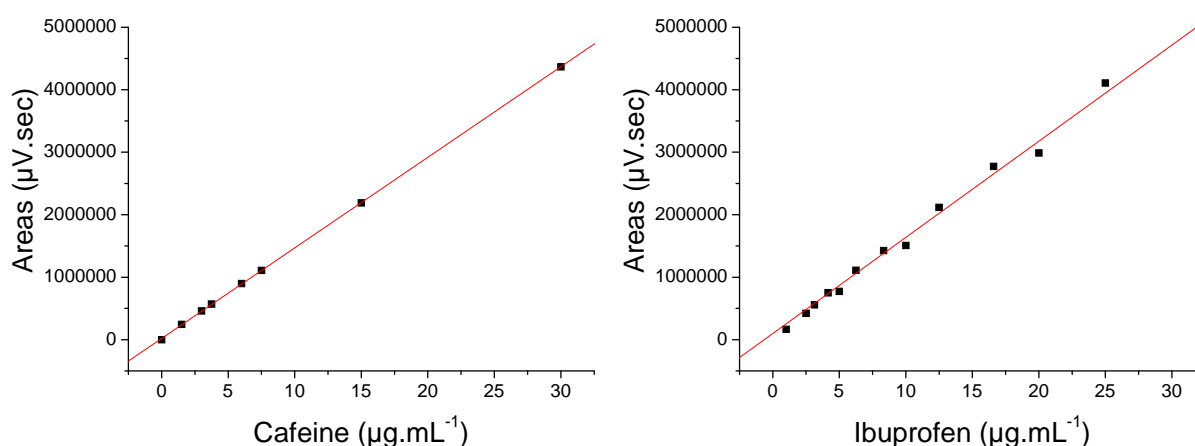


Figure S4. Calibration plot of standard caffeine (left) and ibuprofen (right) by HPLC method.

The standard calibration curve showed a very good correlation coefficient > 0.99 . Chromatogram of standard solutions showed a retention time of 3.6 min (caffeine) or 4.9 min (ibuprofen) and characteristic UV-Vis spectrum were observed with an absorption maximum at 273 nm (caffeine) and 220 nm (ibuprofen) (Figure S5).

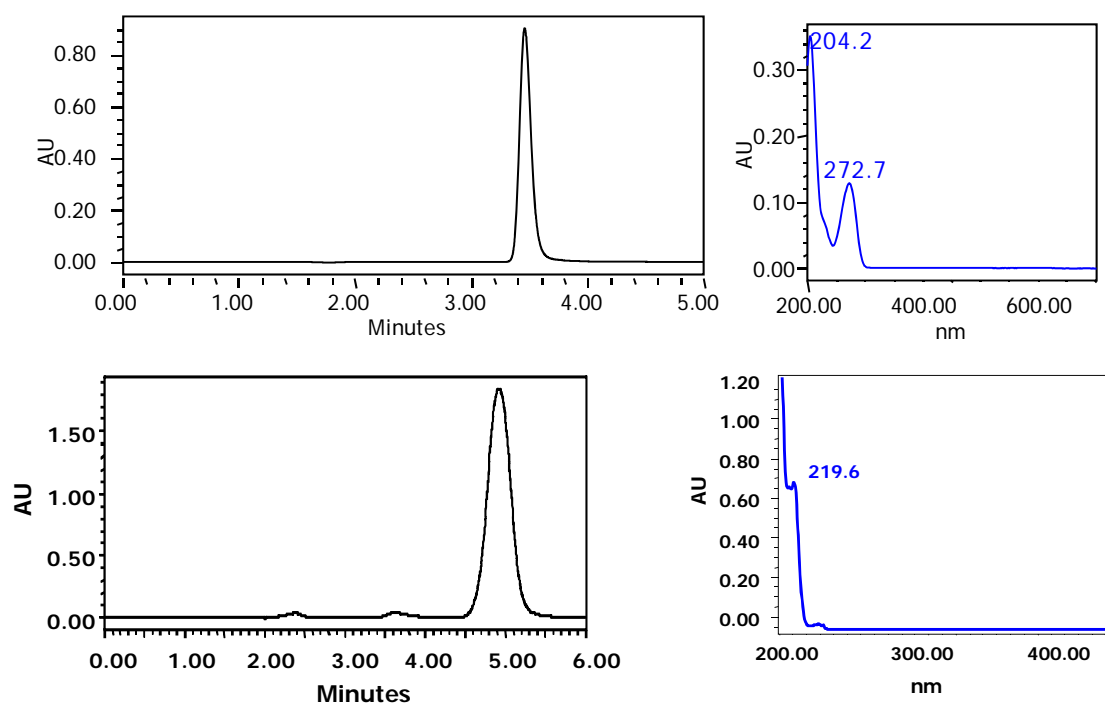


Figure S5. On the left: Chromatograms of standard solutions of caffeine (on the top) and ibuprofen (on the bottom) with a retention time of respectively 3.6 and 4.9 min. On the right: UV-Vis spectra with an absorption maximum at 272 nm (caffeine, top) and 219.6nm (ibuprofen, bottom).

API payloads

Table S3. Caffeine and ibuprofen payloads in the different MOFs estimated by different techniques (HPLC, TGA and elemental analysis)

UiO-66	Caffeine Payloads %			Ibuprofen Payloads %		
	HPLC	TGA	EA	HPLC	TGA	EA
H	22.4±3.4	24	26	34.2±5.5	36.7±0.9	37
Br	21.2±0.7	22	21	17.0±2	16.8±0.2	16
NH₂	13.2±0.2	14	9	28.3±0.4	30±1.5	29
NO₂	10±1.0	7.5	8	15.8±0.8	16±0.5	14
Cl	12.4±0.0	12	14	13.2±0.4	14.2±0.4	13
2CF₃	14.5±3.1	12	13	9.8±1.5	13.2±0.9	11
CH₃	22.5±4.5	22	23	13.4±1.4	12.3±0.7	14
2CH₃	25.8±9.0	24	24	22.3±0.7	21.5±0.4	20
2OH	15.8±4.9	10	14	19±2.7	18.2±0.1	17

3. Computational details: QSAR methodology

Dataset and calculation of the molecular descriptors. The dataset contains a set of 9 functionalized UiO-66(Zr) materials with their caffeine or ibuprofen encapsulation. 4 nanomaterials descriptors and 28 molecular descriptors were considered to build QSAR models. Both types of descriptors were calculated with the Materials Studio software.⁶ The descriptors for the periodic solids were calculated from the crystal structures of each functionalized UiO-66(Zr). They correspond to the density of the materials, the accessible solvent surface area using nitrogen as a probe molecule with a diameter of 3.681 Å,⁷ the free volume and the pore diameter. The molecular descriptors were calculated from each individual functionalized organic linker present in the material, including topological, structural, thermodynamic and electrotopological state keys descriptors.

Variable selection and model building. Multilinear regression (MLR) method implemented in Weka 3.6.2 program⁸ have been used, after the elimination of two descriptors with no variability. The advantage of the MLR approach compared to non linear methods, such as neural networks (NN) or support vector machine (SVM),^{9,10,11,12} relies on its ability to derive easily interpretable mathematical QSAR model that corresponds well with the objective of this study. QSAR individual models based on the selection of 1, 2 or 3 descriptors among this set of 30 descriptors, were further built using this MLR method. For each of the so-generated 4525 models, resulting from the ${}^{30}C_1 + {}^{30}C_2 + {}^{30}C_3$

combinations, the leave-one-out (LOO) cross-validation approach was employed to internally validate their robustness. Indeed, the squared determination coefficient R^2 , the squared cross-validation correlation coefficient Q^2 and the squared root mean square error $RMSE$, were estimated for each model using the following expressions (Equations 1-3):

$$R^2 = 1 - \frac{\sum (y_{train} - y_{exp})^2}{\sum (y_{exp} - \bar{y}_{exp})^2} \quad (\text{Eq. 1})$$

$$Q^2 = 1 - \frac{\sum (y_{pred} - y_{exp})^2}{\sum (y_{exp} - \bar{y}_{exp})^2} \quad (\text{Eq. 2})$$

$$RMSE = \sqrt{\frac{\sum (y_{pred} - y_{exp})^2}{n}} \quad (\text{Eq. 3})$$

where y_{train} and y_{pred} correspond to the calculated (training) and predicted (LOO) property values, y_{exp} is the experimental value, \bar{y}_{exp} is the averaged value over the whole experimental data and n is the number of samples present in the dataset.

The validation of the individual QSAR models was also ensured using a y -randomization strategy, well detailed by Karki and Kulkarni.¹³ It consisted of testing if the MLR models are generated just by pure statistical chance wherein some molecular descriptors with no real significance would show good correlation with the property of interest. To that purpose, the validity of the models was checked by permutation tests: additional models were generated for 100 randomly reordered encapsulation loading property vector. The Q^2 were calculated for all the so-generated random models and further compared, using appropriate histogram, to the value obtained for the original model built from the real encapsulation capacity.

References

- ¹ Cavka, J. H.; Jakobsen, S.; Olsbye, U.; Guillou, N.; Lamberti, C.; Bordiga, S.; Lillerud, K. P. *J. Am. Chem. Soc.* **2008**, *130*, 13850.
- ² Barcia, P. S.; Guimaraes, D.; Mendes, P. A. P.; Silva, J. A. C.; Guillerm, V.; Chevreau, H.; Serre C.; Rodrigues, A. E. *Microporous Mesoporous Mater.* **2011**, *139*, 67.
- ³ Kandiah, M.; Nilsen, M.H.; Usseglio, S.; Jakobsen, S.; Olsbye, U.; Tilset, M.; Larabi, C.; Quadrelli, E. A.; F. Bonino and Lillerud, K. P. *Chem. Mater.* **2010**, *22*, 6632.
- ⁴ Zlotea, C.; Phanon, D.; Mazaj, M.; Heurtaux, D.; Guillerm, V.; Serre, C.; Horcajada, P.; Devic, T.; Magnier, E.; Cuevas, F.; Férey, G.; Llewellyn P. L.; Latroche, M. *Dalton Trans.* **2011**, *40*, 4879.
- ⁵ Guillerm, V. *Synthesis, Functionalisation and Adsorption Properties of New Hybrid Porous Solids*, in Institute Lavoisier. **2011**, Université de Versailles Saint Quentin en Yvelines: Versailles p. 238.

- ⁶ Materials Studio, QSAR/Accelrys, Materials Studio, San Diego, CA, USA, 4.3.0.0 ed., **2008**.
- ⁷ Yazaydin, A.O.Z.R.; Snurr, R. Q.; Park, T.-H.; Koh, K.; Liu, J.; LeVan, M. D.; Benin, A. I.; Jakubczak, P.; Lanuza, M.; Galloway, D. B.; Low J. J.; Willis, R. R. *J. Am. Chem. Soc.* **2009**, *131*, 18198.
- ⁸ Hall, M.; Frank, E.; Holmes, G.; Pfahringer, B.; Reutemann, P.; Witten, I.H. *The WEKA Data Mining Software: An Update*, 3.6.2 ed., **2009**.
- ⁹ Shen, J.; Cheng, F.; Xu, Y.; Li, W.; Tang, Y. *J. Chem. Inf. Model.* **2010**, *50*, 1034.
- ¹⁰ Reddy, A. S.; Kumar, S.; Garg, R. *J. Mol. Graph. Model.* **2010**, *28*, 852.
- ¹¹ Katritzky, A. R.; Kuanar, M.; Slavov, S.; Hall, C. D.; Karelson, M.; Kahn, I.; Dobchev, D.A. *Chem. Rev.* **2010**, *110*, 5714.
- ¹² Hewitt, M.; Cronin, M. T. D.; Enoch, S. J.; Madden, J.C.; Roberts, D.W. ; Dearden, J.C. *J. Chem. Inf. Model.* **2009**, *49*, 2572.
- ¹² Burden, F. R.; Ford, M. G.; Whitley, D. C.; Winkler, D. A. *J. Chem. Inf. Comput. Sci.* **2000**, *40*, 1423-1430.
- ¹³ Karki, R. G.; Kulkarni, V. M. *Biorg. Med. Chem.* **2001**, *9*, 3153.